Chemistry and Materials

The Center for Science Innovation

Research Article

Chem. Mater. 2 (1) 2023, 1-7

Electrodeposition of CoNi Cocatalyst to Enhance Ethanol Electrooxidation of Zn-doped Cu_2O-Cu Photocatalyst

Alfian Putra Utama[1,2] *, Afrizal[2]

[1]PT Centa Brasindo Abadi Chemical Industry, Jl. Raya Cikande Rangkasbitung, KM 10, Serang, Banten, Indonesia

[2]Department of Chemistry, Faculty of Mathematics and Natural Sciences, Universitas Negeri Jakarta, Jl. Rawamangun Muka, Jakarta 13220, Indonesia

*Corresponding author: alfianvanputra@gmail.com

Received
24 September 2022

Received in revised form
6 January 2023

Accepted
26 January 2023

Published online
27 February 2023

DOI
https://doi.org/10.56425/cma.v2i1.44

Abstract

In this research, the electrooxidation of ethanol was catalyzed using Zn-doped Cu_2O-Cu/CoNi heterostructure syntesized using an electrodeposition method. Potential deposition of CoNi cocatalyst was varied to obtain the highest photo-electrochemical performance and photocatalytic activity of Zn-doped Cu_2O-Cu/CoNi. The photoelectrochemical properties and photocatalytic activity investigated by electrochemical impedance spectroscopy, linear sweep voltammetry, and cyclic voltammetry. The increase of deposition potential from -1.3 V to -1.75 V increased the ethanol oxidation reaction. Zn-doped Cu_2O-Cu/CoNi -1.75 V electrode showed superior photocatalytic activity for the ethanol electrooxidation compared to other electrodes. This photocatalyst showed a high photocurrent density of 22.47 mA/cm^2. Moreover, cyclic voltammetry tests up to 100 cycles indicated that CoNi deposition potential at -2 V increased the long-term stability of the photocatalyst against the poisoning species than other electrodes. The fraction of CoNi enhanced CO tolerance and contributed to the higher specific activity towards ethanol electrooxidation. An excess number of CoNi at -2 V was found to decrease photocatalytic activity but increase the photostability of the material.

Keywords: electrodeposition, ethanol electrooxidation, photocatalyst, cocatalyst, deposition potential, Zn-doped Cu_2O-Cu/CoNi, photostability

1. Introduction

Fossil fuel consumption increases carbon dioxide (CO_2) emissions into atmosphere that caused several negative environmental impacts, such as global energy shortages and greenhouse effect [1-3]. Therefore, studies on renewable energy technologies are important. Currently, direct ethanol fuel cells (DEFC) have emerged as an effective strategy with low costs energy. The development of DEFC is still constrained by low efficiency, due to the formation of by-products so that the electrooxidation kinetics of ethanol becomes slow and durability is low [4]. The use of nanostructured photo-catalysts shows high electrooxidation activity of ethanol with long durability because the catalytic activity of electrodes increases significantly.

In term of photocatalyst materials, metal-doped Cu_2O like Zn has shown better photocatalytic activity. Previous studies showed that Zn-doped Cu_2O has a good impact such as lattice shrinkage, band-gap adjustment, surface defects, increased photoelectrochemical properties, and suppressing recombination electron-hole [5–14]. On the other hand, copper metal and its oxide (Cu_2O-Cu) have unique catalytic properties, high abundance, high thermal and electrical conductivity, low toxicity level, cost-effective, and a small band gap energy with the range of 1.2–2.2 eV so that it efficiently acts on the visible region and absorbs more photon energy to induce redox reactions and promises for the conversion of solar power into electricity or chemical energy [15–17]. However, pure Cu_2O has a low electrical power conversion efficiency of 2% [17]. In theory, Cu_2O has a light-to-H_2 (STH) efficiency at water electrolysis of 18% on the 1.5 AM spectrum for solar cells [18]. Cu_2O is also limited by the light-induced recombination electron-hole pairs, poor durability, unstable in humid air and easily oxidizes to CuO [15,20–21]. Therefore, in this study the Zn-doped composite Cu_2O-Cu was developed to increase the electrooxidation activity of

ethanol with longer durability. The use of cocatalysts to improve photocatalysts performance and stability is interesting because it can trap charges and induce electron-holes separation by creating interfaces with photocatalysts. In addition, cocatalysts are alternative locations of reactions thus preventing photo corrosion of photocatalysts [20]. Precious metals such as Pt, Rh, Pd Au, and RuO_2 oxides are often used as cocatalysts. However, these metals are expensive and rare [21]. Recently, cocatalyst of bimetallic CoNi was reported to have superior performance at various reactions, such as alcohol dehydrogenation, nitrile hydrogenation, methane reshaping, and ethanol oxidation reaction [22]. In previous studies, CoNi with Ca-γ-Al_2O_3 was used for ethanol oxidation reactions that produce hydrogen [23]. Then, perovskite-type oxide (PTO) coated with CoNi was used in the Steam Reforming of Ethanol (SRE) reaction [24]. PTO with CoNi has better performance than one without CoNi. Zhao et al. [21] reported that the presence of bimetal CoNi in Al_2O_3 produce a highest stability in ethanol conversion compared to Al_2O_3/Co and Al_2O_3/Ni. This indicate a possible synergistic effect between CoNi cocatalysts to improve photocurrent performance and stability of Zn-doped Cu_2O-Cu as photocatalysts in ethanol electro-oxidation. There has been no study on the Zn-doped Cu_2O-Cu nanocomposite coated with CoNi cocatalyst for ethanol electrooxidation reactions. Therefore, in this study, CoNi cocatalyst was electrodeposited on the Zn-doped Cu_2O-Cu to improve catalytic activity of the photocatalyst. The CoNi was electrodeposited by different deposition potentials. Photocatalytic activity of the Zn-doped Cu_2O-Cu/CoNi was evaluated toward ethanol electrooxidation reaction.

2. Materials and Method

2.1 Materials

All chemical used in this studies were ACS grade supplied by Merck, namely cupric sulfate pentahydrate ($CuSO_4{\cdot}5H_2O$), zinc sulfate heptahydrate ($ZnSO_4{\cdot}7H_2O$), sodium sulfate (Na_2SO_4), boric acid (H_3BO_3), cobalt sulfate heptahydrate ($CoSO_4{\cdot}7H_2O$), and nickel sulfate hexa-hydrate ($NiSO_4{\cdot}6H_2O$). The substrate used in this work was ITO coated polyethylene terephthalate (PET).

2.2 Zn-doped Cu_2O-Cu/CoNi preparation

Zn-doped Cu_2O-Cu was synthesized on ITO substrate by galvanostatic with a deposition current of -1 mA/cm^2 that carried out in a three-electrode cell using Ag/AgCl as a reference electrode, and platinum electrode as a auxiliary electrode, respectively. The electrodeposition was controlled by a potentiostat EDAQ ER466 at 60^{o}C for 1 hourThe Zn-doped Cu_2O-Cu deposition was conducted in an electrolyte containing 0.025 M $CuSO_4{\cdot}5H_2O$, 0.014 M $ZnSO_4{\cdot}7H_2O$, and 0.2 M Na_2SO_4. Modification of the Zn-doped Cu_2O-Cu nanocomposite with CoNi cocatalyst was conducted by potensiostatic technique with different potentials i.e., -1.3 V, -1.5 V, -1.75 V, and -2 V. The deposition was carried out in a three-electrode cell and controlled by a potentiostat EDAQ ER466. The CoNi were deposited by immersing Zn-doped Cu_2O-Cu film into aqueous solution containing 0.4 M H_3BO_3, 0.05 M $CoSO_4{\cdot}7H_2O$, and 0.1 M $NiSO_4{\cdot}6H_2O$ at room temperature for 45 seconds.

2.2 Characterization of material

X-ray diffraction patterns were acquired using a PANalytical AERIS XRD to study the composition and structure of the samples. Field emission scanning electron microscope (FESEM, Inspect F50) equipped with an energy dispersive X-ray (EDAX, TSL AMETEK) were used to investigate morphology and chemical compositions of the Zn-doped Cu_2O-Cu/CoNi.

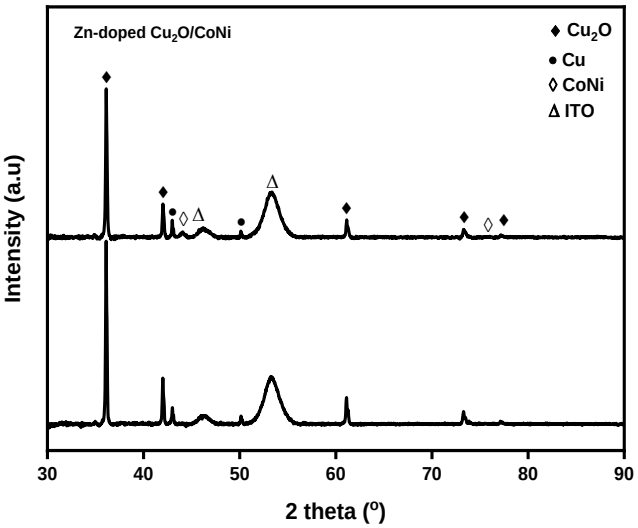

Figure 1. XRD diffraction of Zn-doped Cu_2O-Cu/CoNi with different deposition potentials of CoNi.

2.3 Electrochemical measurements

Photoelectrochemical and photocatalytic activity measurements were conducted using electrochemical impedance spectroscopy (EIS), linear sweep voltammetry (LSV), and cyclic voltammetry (CV) methods. All measurements were performed using a standard three-electrode system were performed using an electrochemical workstation (CS310) with CS Studio 5 software equipped with simulated solar irradiation (AM 1.5 G). These EIS were recorded in 0.5 M KCl electrolyte in the frequency region of 0.1–10^4 Hz. The LSV curves were recorded in 0.5 M Na_2SO_4 electrolytes under a bias voltage of between −0.5 V and 1.5 V vs Ag/AgCl at a scan rate of 10 mVs^{-1}. The CV were recorded in 1 M ethanol + 0.1M NaOH electrolytes under a bias voltage of between −0.2 V and 0.5 V vs Ag/AgCl. The EIS and LSV scans were recorded with and without irradiation conditions.

3. Results and Discussion

3.1 Characterization analysis

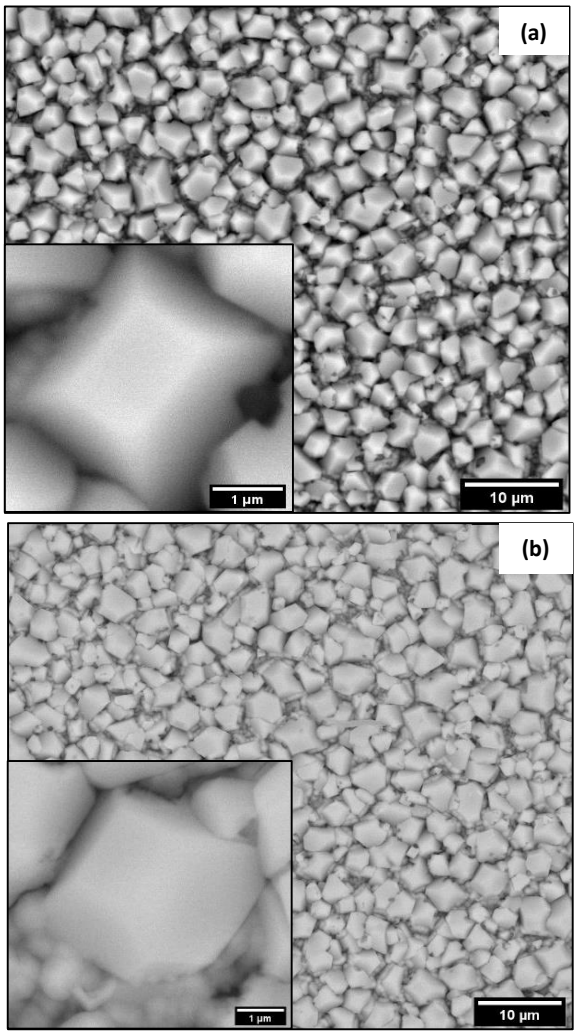

Figure 2. FESEM morphological representation of Zn-doped Cu_2O-Cu/CoNi with different CoNi deposition potentials of (a) -1.75 V (b) -2 V.

The XRD patterns of Zn-doped Cu_2O-Cu/CoNi shown in Fig. 1 confirmed the formation of Zn-doped Cu_2O-Cu/CoNi. In the Zn-doped Cu_2O-Cu/CoNi -1.5, diffraction peaks at 2-theta of 36.46°, 42.31°, 61.4°, 73.52°, 77.36° correspond to the reflection of (111), (200), (220), (311), (222) planes of the cuprite Cu_2O, respectively (JCPDS No. 01-071-3645). While peaks at 2-theta of 43.33°, 50.45° correspond to the reflection of (111), (200) planes of the copper Cu (JCPDS No. 01-071-4609). When the CoNi deposition potential is increased to -2 V, the weak diffraction peaks appeared at 2-theta of 44.1° and 76.1° that could be attributed to the CoNi (JCPDS No. 01-074-5694). The presence of CoNi is also confirmed by the FESEM measurement shown in Fig 2.

Based on the FESEM micrograph, the Zn-doped Cu_2O-Cu is truncated octahedral. The CoNi are grown around the Zn-doped Cu_2O-Cu and have an almost spherical morphology. In this study, the difference CoNi deposition potential affected the Zn-doped Cu_2O-Cu/CoNi surface density. The more negative the CoNi deposition potential, higher surface density of the sample. This result is supported by the EDX data in Fig. 3, which shows that the negative the deposition potential, the more the composition of the Co and Ni elements increased. At -1.75V Co and Ni elements appeared in the EDX spectrum of 0.91% (Co) and 0.92% (Ni) Wt. %. CoNi growth of 3.86% (Co) and 3.93% (Ni) Wt. % when the deposition potential was -2 V. This is because the negative potential increased the current density that increased the number of deposited CoNi crystals [25].

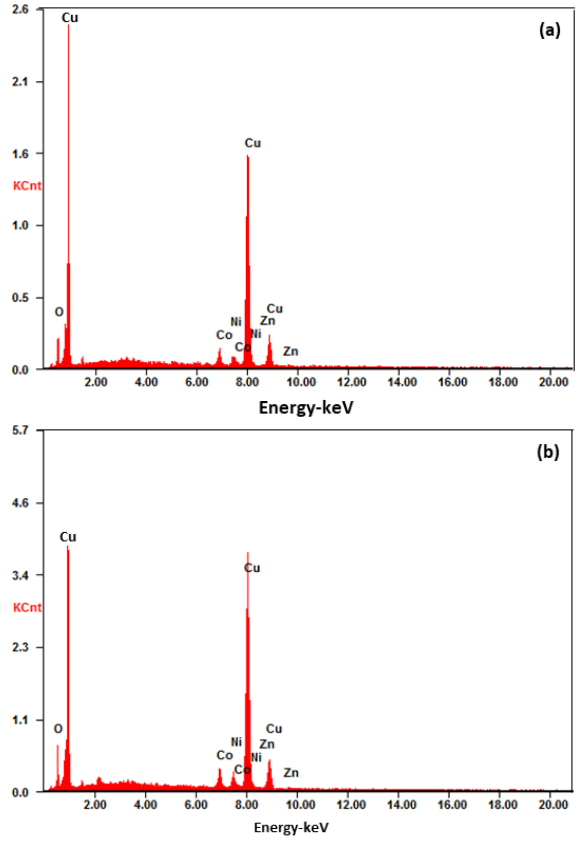

Figure 3. EDX spectrum of Zn doped Cu_2O-Cu/CoNi with different CoNi deposition potentials of (a) -1.75 V (b) -2 V.

3.2 Photoelectrochemical analysis

The efficiency of separation and charge carriers transport and photocurrent of the Zn-doped Cu_2O-Cu/CoNi were tested under visible light irradiation. The Nyquist plot shown in Fig. 4 indicated that the increase of CoNi deposition potential from -1.3 V to 1.75 V decreased the resistance charge transfer (R_{ct}) values. Meanwhile the R_{ct} was found to increase at -2V. This is due to the increased of CoNi deposit. The thicker CoNi deposit can cover light hitting the Zn-doped Cu_2O-Cu surface and reducing the

production of h^+ and e^- [26]. In this study, the lowest R_{ct} belonged to the Zn-doped Cu_2O-Cu/CoNi sample -1.75 V. This is supported by the EIS measurement of the Zn-doped Cu_2O-Cu/CoNi -1.75 (Fig. 4).

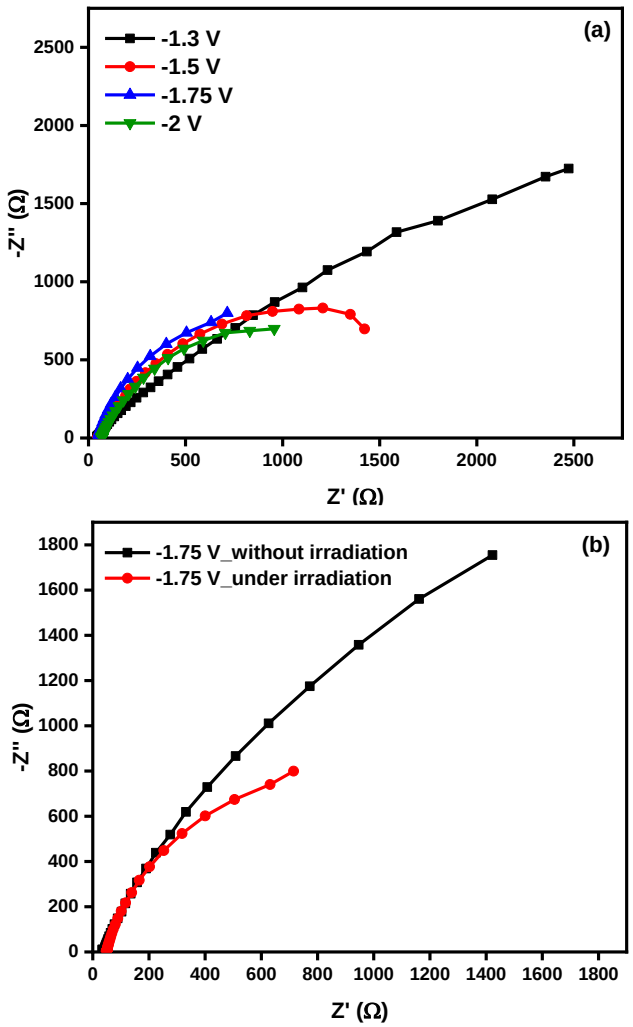

Figure 4. Nyquist plots of Zn-doped Cu_2O-Cu/CoNi (a) with difference CoNi deposition potentials and (b) the plot recorded with and without irradiation.

Fig. 4b shows that R_{ct} with and without irradiation increased significantly from 2150 Ω to 5049 Ω because the photon energy generated from irradiation can make Zn-doped Cu_2O-Cu/CoNi surface conductive and increase the carrier density thereby accelerating charge transfer at the electrode and solution interfaces [27–28]. The resistance directly affects charge separation efficiency as indicated by the photocurrent density value (Fig. 5a-b). Based on the data, Zn-doped Cu_2O-Cu/CoNi -1.75 which has the lowest resistance showed a high photocurrent value of 22.47 mA/cm^2. The photocurrent increases with the increase of CoNi deposition potential towards the cathodic direction from -1.3 V to -1.75 V and decreases at -2V. In this case, the CoNi cocatalyst plays the role an electron donor. An increase in the amount of CoNi (electron donors) can increase the electric field and high efficiency charge separation [29]. However, increase amount of CoNi over Zn-doped Cu_2O-Cu may reduce the limiting current that may be caused by the shadowing effect [30]. Under irradiation, photocurrent was higher compared to that obtained without irradiation. This is due to the semi-conductor characteristics of the Cu_2O which shows good electron transfer kinetics with irradiation.

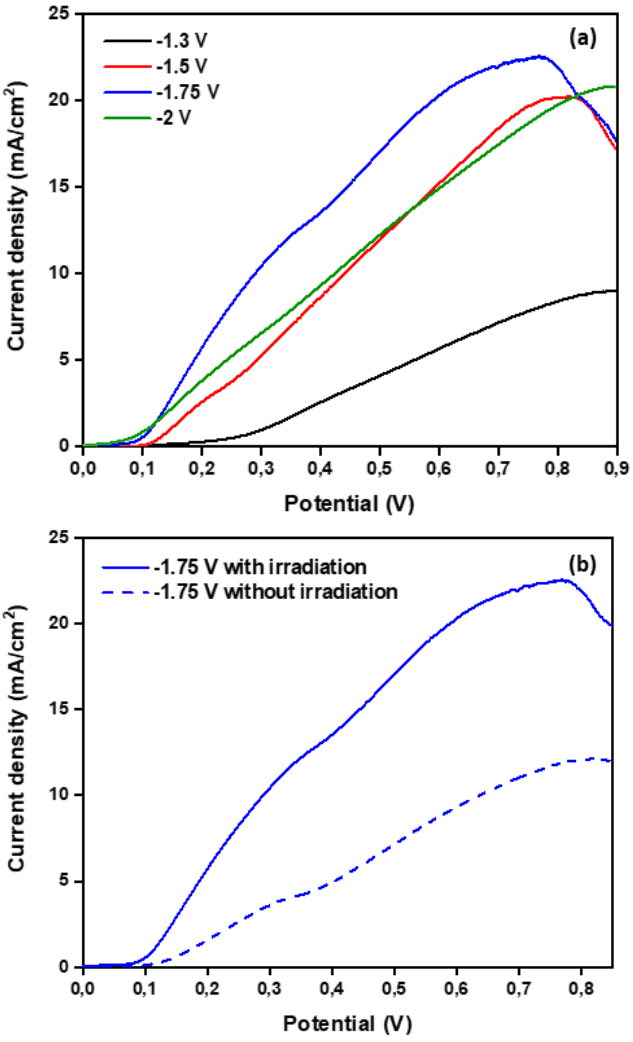

Figure 5. LSV curves of Zn-doped Cu_2O-Cu/CoNi (a) of difference deposition potential CoNi, and (b) recorded with and without irradiation.

3.3 Catalytic activity test toward ethanol electrooxidation

Ethanol electrooxidation tests were performed to evaluate the photocatalytic performance of Zn-doped Cu_2O-Cu/CoNi. It is known that the ethanol electro-oxidation range is 0 V to 0.5 V ethanol [31]. The cyclic voltammogram show peak between 0.2 and 0.4 V on forward scan. This peak is derived from adsorption of hydroxyl groups on the photocatalyst surface. In the back-

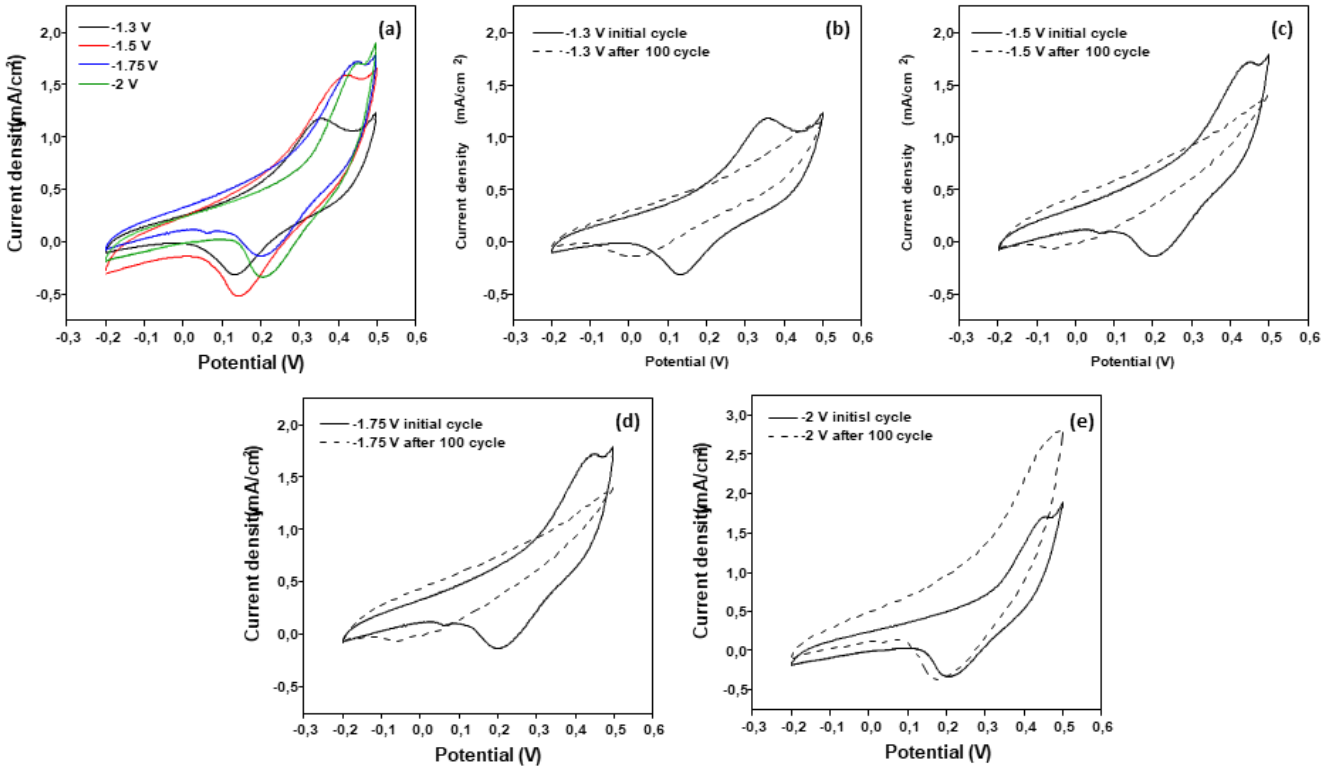

Figure 6. Cyclic voltammetry of Zn-doped Cu_2O-Cu/CoNi with difference CoNi deposition potential in ethanol electrooxidation process (a) initial cycle and (b)-(e) comparison of initial and after 100 cycles.

ward scans an oxidation peak appeared between 0.1 V and 0.2 V, representing the electrochemical oxidation of CO_{ads} and other absorbed species that are not fully oxidized during forward scan. This is because OH_{ads} species converted toxic species (such as CO) into CO_2 or other non-toxic products on CoNi surfaces [18].

In general, the smaller the ratio of peak density backward scan (j_b) current to forward scan (j_f) indicate the better poisoning resistance of the photocatalysts in the ethanol oxidation reaction. The different of CoNi deposition potentials shown in Fig. 6 affected the j_b/j_f value. Based on the data, Zn-doped Cu_2O-Cu/CoNi -1.75 which has the highest photoelectrochemical properties has superior photocatalytic activity for electrooxidation of ethanol in alkaline media and better poisoning resistance compared with other Zn-doped Cu_2O-Cu/CoNi becauce of the smallest j_b/j_f ratio. The known electrooxidation reaction of ethanol through 12 electrons transfer is shown in Equation (1).

$$C_2H_5OH + 12OH^- \rightarrow 2CO_2 + 9H_2O + 12e^- \quad (1)$$

Unlike the Zn-doped Cu_2O-Cu/CoNi -1.75 V that has the highest photocatalytic activity, after 100 cycles of Zn-doped Cu_2O-Cu/CoNi -2 it has the best level of photostability (Fig. 5e). Photostability is quantified as the percentage of photocurrent at the end of the cycle (J) compared to at the initial cycle (J_0). This result related to the number of CoNi deposited on the Zn-doped Cu_2O-Cu. A thicker deposit of CoNi can indeed cover the Zn-doped Cu_2O-Cu that increase the stability of the photocorosion [26]. Therefore, in this case, Zn-doped Cu_2O-Cu/CoNi -2 V has high stability in the ethanol electrooxidation process.

4. Conclusion

The CoNi cocatalyst was electrodeposited over Zn-doped Cu_2O-Cu. Based on results of the load carrier separation and transport efficiency tests showed that the increase CoNi deposition potential towards the cathodic direction from -1.3 V to -1.75 V increased the photocatalytic performance of the Zn-doped Cu_2O-Cu/CoNi. This is because number of CoNi deposit increased with the increase deposition potential. However, an excess number of CoNi at -2 V can block light exposure on Zn-doped Cu_2O-Cu surface and reduced electron and hole production which is decreases photocatalytic activity. On the other hand, the number of CoNi is found to contribute to the increase of photostability of the Zn-doped Cu_2O-Cu. In this study, the optimum CoNi cocatalyst deposition potential for ethanol electrooxidation was obtained at -1.75 V, while best photostability was produced with the deposition potential of -2 V.

Acknowledgement

This research was supported by Direktorat Riset, Teknologi dan Pengabdian kepada Masyarakat Kemendikbudristek

under PTKN's research scheme (contract number: 6/E5/PG.02.00.PT/LPPM/V/2022). The author also thank to the Center for Science Innovation that supported this work by facilitating the electrochemical workstation.

References

[1] N. Sazali, Emerging technologies by hydrogen: A review, *Int. J. Hydrogen Energy*. **45** (2020) 18753–18771. https://doi.org/10.1016/j.ijhydene.2020.05.021.

[2] Y. Turap, I. Wang, T. Fu, Y. Wu, Y. Wang, W. Wang, Co–Ni alloy supported on CeO_2 as a bimetallic catalyst for dry reforming of methane, *Int. J. Hydrogen Energy*. **45** (2020) 6538–6548. https://doi.org/10.1016/j.ijhydene.2019.12.223.

[3] S. Cao, Y. Li, B. Zhu, M. Jaroniec, J. Yu, Facet effect of Pd cocatalyst on photocatalytic CO_2 reduction over g-C_3N_4, *J. Catal.* **349** (2017) 208–217 https://doi.org/10.1016/j.jcat.2017.02.005.

[4] Y. Zheng, X. Wan, X. Cheng, K. Cheng, Z. Liu, Z. Dai, Advanced catalytic materials for ethanol oxidation in direct ethanol fuel cells, *Catalysts*. **10** (2020). https://doi.org/10.3390/catal10020166.

[5] S. Budi, D. Indrawati, M. Arum, Yusmaniar, Electrodeposition and photoelectrochemical response of Zn-doped Cu_2O, *AIP Conf. Proc.* **2342** (2021). https://doi.org/10.1063/5.0045470.

[6] T.G. Kim, H.J. Lee, H. Ryu, W.J. Lee, Effects of Zn amount on the properties of Zn-Zu_2O composite films grown for PEC photoelectrodes by using electrochemical deposition, *J. Korean Phys. Soc.* **67** (2015) 1273–1277. https://doi.org/10.3938/jkps.67.1273.

[7] L. Zhang, D. Jing, L. Guo, X. Yao, In situ photochemical synthesis of Zn-Doped Cu_2O hollow microcubes for high efficient photocatalytic H_2 Production, *ACS Sustain. Chem. Eng.* **2** (2014) 1446–1452. https://doi.org/10.1021/sc500045e.

[8] F. Hu, Y. Zou, L. Wang, Y. Wen, Y. Xiong, Photostable Cu_2O photoelectrodes fabricated by facile Zn-doping electrodeposition, *Int. J. Hydrogen Energy*. **41** (2016) 15172–15180. https://doi.org/10.1016/j.ijhydene.2016.06.262.

[9] F. Ye, X.Q. Su, X.M. Cai, Z.H. Zheng, G.X. Liang, D.P. Zhang, J.T. Luo, P. Fan, The electrical and thermoelectric properties of Zn-doped cuprous oxide, *Thin Solid Films*. **603** (2016) 395–399. https://doi.org/10.1016/j.tsf.2016.02.037.

[10] X. Yu, J. Zhang, J. Zhang, J. Niu, J. Zhao, Y. Wei, B. Yao, Photocatalytic degradation of ciprofloxacin using Zn-doped Cu_2O particles: Analysis of degradation pathways and intermediates, *Chem. Eng. J.* **374** (2019) 316–327. https://doi.org/10.1016/j.cej.2019.05.177.

[11] K. Lee, C.H. Lee, J.Y. Cheong, S. Lee, I.D. Kim, H.I. Joh, D.C. Lee, Expanding depletion region via doping: Zn-doped Cu_2O buffer layer in Cu_2O photocathodes for photoelectrochemical water splitting, *Korean J. Chem. Eng.* **34** (2017) 3214–3219. https://doi.org/10.1007/s11814-017-0225-8.

[12] C.P. Goyal, D. Goyal, V. Ganesh, N.S. Ramgir, M. Navaneethan, Y. Hayakawa, C. Muthamizhchelvan, H. Ikeda, S. Ponnusamy, Improvement of Photocatalytic Activity by Zn Doping in Cu_2O, *Phys. Solid State*. **62** (2020) 1796–1802. https://doi.org/10.1134/S1063783420100091.

[13] C. Zhu, M.J. Panzer, Synthesis of Zn:Cu_2O Thin Films Using a Single Step Electrodeposition for Photovoltaic Applications, *ACS Appl. Mater. Interfaces*. **7** (2015) 5624–5628. https://doi.org/10.1021/acsami.5b00643.

[14] Y. Yuan, L.M. Sun, H. Gao, S. Mo, T. Xu, L. Yang, W.W. Zhan, Engineering a highly improved porous photo-catalyst based on Cu_2O by a synergistic effect of cation doping of Zn and carbon layer coating, *Inorg. Chem.* **59** (2020) 16010–16015. https://doi.org/10.1021/acs.inorgchem.0c02547.

[15] S. Muneekaew, K.C. Chang, A. Kurniawan, Y. Shirosaki, M.J. Wang, Microwave plasma treated composites of Cu/Cu_2O nanoparticles on electrospun poly(N-vinylpyrrolidone) fibers as highly effective photocatalysts for reduction of organic dyes and 4-nitrophenol, *J. Taiwan Inst. Chem. Eng.* **107** (2020) 171–181. https://doi.org/10.1016/j.jtice.2019.11.008.

[16] Y.T. Gaim, G.M. Tesfamariam, G.Y. Nigussie, M.E. Ashebir, Synthesis, characterization and photocatalytic activity of n-doped Cu_2O/ZnO nanocomposite on degradation of methyl red, *J. Compos. Sci.* **3** (2019). https://doi.org/10.3390/jcs3040093.

[17] A. Yunusa, A.O. Musa, Copper (I) oxide (Cu_2O) based solar cells - A review, (2017).

[18] I. V. Bagal, N.R. Chodankar, M.A. Hassan, A. Waseem, M.A. Johar, D.H. Kim, S.W. Ryu, Cu_2O as an emerging photocathode for solar water splitting - A status review, *Int. J. Hydrogen Energy*. **44** (2019) 21351–21378. https://doi.org/10.1016/j.ijhydene.2019.06.184.

[19] Y. Fu, Q. Li, J. Liu, Y. Jiao, S. Hu, H. Wang, S. Xu, B. Jiang, In-situ chemical vapor deposition to fabricate Cuprous oxide/copper sulfide core-shell flowers with boosted and stable wide-spectral region photocatalytic performance, *J. Colloid Interface Sci.* **570** (2020) 143–152. https://doi.org/10.1016/j.jcis.2020.02.110.

[20] V.A. Online, W. Yin, Z. Li, Y. Xiong, RSC Advances, (2016). https://doi.org/10.1039/b000000x.

[21] J. Zhao, X. Yan, N. Zhao, X. Li, B. Lu, X. Zhang, H. Yu, RSC Advances cocatalyst system consisting of $ZnIn_2S_4$ and $In(OH)_3$, *RSC Adv.* **8** (2018) 4979–4986. https://doi.org/10.1039/C7RA12586K.

[22] M. Muñoz, S. Moreno, R. Molina, The effect of the absence of Ni, Co, and Ni-Co catalyst pretreatment on catalytic activity for hydrogen production via oxidative steam reforming of ethanol, *Int. J. Hydrogen Energy*. **39** (2014) 10074–10089. https://doi.org/10.1016/j.ijhydene.2014.04.131.

[23] L. Chen, C. Kai, S. Choong, Z. Zhong, L. Huang, Z. Wang, J. Lin, Support and alloy effects on activity and product selectivity for ethanol steam reforming over supported nickel cobalt catalysts, *Int. J. Hydrogen Energy*. **37** (2012) 16321–16332. https://doi.org/10.1016/j.ijhydene.2012.02.119.

[24] Z. Wang, C. Wang, S. Chen, Y. Liu, ScienceDirect Co-Ni bimetal catalyst supported on perovskite-type oxide for steam reforming of ethanol to produce hydrogen, *Int. J. Hydrogen Energy*. **39** (2014) 5644–5652. https://doi.org/10.1016/j.ijhydene.2014.01.151.

[25] S. Jeon, G. Song, D.H. Hur, Effects of Deposition Potentials on the Morphology and Structure of Iron-Based Films on Carbon Steel Substrate in an Alkaline Solution, **2016** (2016).

[26] V. Soni, C. Xia, C. Kui, V. Nguyen, D. Le, T. Nguyen, P. Singh, P. Raizada, Advances and recent trends in cobalt-based cocatalysts for solar-to-fuel conversion, *Appl. Mater. Today*. **24** (2021) 101074. https://doi.org/10.1016/j.apmt.2021.101074.

[27] P. Ghamgosar, F. Rigoni, S. You, I. Dobryden, M.G. Kohan, A.L. Pellegrino, I. Concina, N. Almqvist, G. Malandrino, A. Vomiero, ZnO-Cu_2O core-shell nanowires as stable and fast response photodetectors, *Nano Energy*. **51** (2018) 308–316. https://doi.org/10.1016/j.nanoen.2018.06.058.

[28] Y. Yang, D. Xu, Q. Wu, P. Diao, Cu_2O/CuO bilayered composite as a high-efficiency photocathode for photoelectrochemical hydrogen evolution reaction, *Sci. Rep.* **6** (2016) 1–13. https://doi.org/10.1038/srep35158.

[29] G. Iervolino, I. Tantis, L. Sygellou, V. Vaiano, Applied Surface Science Photocurrent increase by metal modification of Fe_2O_3 photoanodes and its effect on photoelectrocatalytic hydrogen production by degradation of organic substances, *Appl. Surf. Sci.* **400** (2017) 176–183. https://doi.org/10.1016/j.apsusc.2016.12.173.

[30] I. Oh, J. Kye, S. Hwang, Fabrication of Metal-Semiconductor Interface in Porous Silicon and Its Photoelectrochemical Hydrogen Production, **32** (2011) 4392–4396.

[31] X. Li, S. Ning, X. Liu, E. Shangguan, C. Wu, J. Li, Z. Wang, Q. Li, Insights into the electrode reaction process of nickel nanoparticles @reduced graphene oxide catalyst for ethanol oxidation in alkaline solution, *Ionics (Kiel).* **25** (2019) 3775–3786. https://doi.org/10.1007/s11581-019-02945-2.